ONLINE SUPPLEMENTARY MATERIAL

Text S1. Sandeel data sources

Length at date data for the lesser sandeel (*Ammodytes marinus*) were compiled from a variety of sources (Table S1). The largest and most consistent data sources were (1) age 0 sandeel data collected weekly between 2000 and 2016 at the MSS coastal ecosystem monitoring site (using an ichtyoplankton1m ringnet in Table S1, referred to as "ringnet" in the model) on the Scottish east coast at Stonehaven (SCObs; http://data.marine.gov.scot/dataset/scottish-coastal-observatory-stonehaven-site), (2) age 0 sandeel data measured from puffin diet on the Isle of May during the breeding season between 2000 and 2016 (full details of methods in Wanless et al. 2018, referred to as "puffins" in the model) and (3) age 0 sandeel data originating from the dedicated annual winter sandeel dredge survey targeting overwintering sandeel in the Firth of Forth (referred to as "dredge" in the model). In addition to these 3 main sources, data on age 0 sandeel caught from plankton samplers (Methot net: referred to as "MT" in the model, Gulf III sampler: referred to as "G3" in the model, pelagic (pelagic net: referred to as "pelagic" in the model and International Young Gadoid Pelagic Trawl: referred to as "PT154" in the model and demersal trawls (referred to as "demersal" in the model) and benthic samplers (modified sandeel dredge referred to as "SDG" for the summer sandeel surveys and "dredge" for the winter dredge surveys) were included (Table S1).

Sandeel abundance indices were derived from the dedicated annual winter (November/December) sandeel dredge survey in years 2000 to 2003 and 2008 to 2016 (ICES 2021). The age 0 index from this winter survey is highly correlated with that estimated from pelagic trawls in June surveys (Régnier et al. 2017). Year-class estimates of age 0 and age 1 from winter surveys are also strongly correlated (ICES 2021). Due to a gap in annual surveys, sandeel abundance indices (age 0 and age 1) were missing for years 2004, 2005, 2006 and 2007. For age 0 abundances, missing values were imputed using the weighted average between predictions of two models. The first model described the relationship between age 0 sandeel abundance and the average mass of age 0 sandeels in puffin loads during chick rearing extracted from Wanless et al. (2018). The relationship was modelled using a linear model with log-transformed age 0 sandeel mass and log-transformed age 0 abundance index and provided a good fit ($F_{1,10} = 17.09$, $R^2 = 0.63$). The second model was a GLM describing variations in the age 0 sandeel abundance index with the overlap index between sandeel hatching and egg production in their copepod prey. The overlap index was extracted from Régnier et al. (2019) and the GLM provided a good fit (pseudo $R^2 = 0.74$). The respective R^2 and pseudo R^2 were use as weights to produce the weighted average between the two model predictions. Missing age 1 abundances were derived from the linear relationship between log-transformed abundance at age 1 at year *y* and log transformed abundance of age 0 at year *y-1* using annual abundance indices estimated in the Firth of Forth during periods 1999-2003 and 2008-2020 ($F_{1,12} = 14.63$, $R^2 = 0.55$).

Table S1. Length at date data (number of individuals) classified by data source.

Year	1m-ringnet	Gulf III	Methot Net	Pelagic trawl	PT154 (pelagic)	Demersal trawl	Dredge	Day Grab	Puffin diet	Total
2000	222			215		20	2023		1732	**4212**
2001	248			95			85		1852	**2280**
2002	2283			238			338		1592	**4451**
2003	1389			167		122	592		2280	**4550**
2004	1277						36		3425	**4738**
2005	517			103					2777	**3397**
2006	504			21					2055	**2580**
2007	402								1541	**1943**
2008	200						920		977	**2097**
2009	63					90	7661		1226	**9040**
2010	140						1105		1266	**2511**
2011	285						449		1729	**2463**
2012	135						554		2228	**2917**
2013	1642	2068	2944		148		702	152	1522	**9178**
2014	184						4079		1375	**5638**
2015	127						1672		2021	**3820**
2016	803						1771		2511	**5085**

Text S2. Seabird data sources

Median annual laying dates came from daily observations of pairs of guillemots and razorbills and observations every five days for kittiwakes and seven days for shags breeding in study plots scattered through the colony (Newell et al. 2015, Table S2). Laying dates of puffins could not be recorded directly because this species is sensitive to disturbance during incubation (Harris & Wanless 2011). Instead laying dates were back-calculated from the annual first hatching dates using a 42 days for the incubation period (Harris & Wanless 2011). Annual values for hatching dates were calculated as the annual date from standardised monitoring of puffin (first), guillemot (median) and razorbill (median). Hatching dates of kittiwake and shag were estimated from their laying dates by adding constants of 27 and 30 days respectively for the incubation periods of these species (https://www.bto.org/understanding-birds/birdfacts). The duration of the chick-rearing period was only available annually with precision in guillemot and razorbill in these populations, so we used a species-specific constant available from the literature to ensure a consistent approach was used across the five species. Fledging dates were therefore calculated by adding average fledging periods to hatching dates (midpoint between minimum and maximum fledging period obtained from the British Trust for Ornithology website: puffin 39 days, kittiwake 43 days, guillemot 21 days, razorbill 19 days, and shag 53 days; https://www.bto.org/understanding-birds/birdfacts; accessed 02/03/2021)

Table S2. Seabird data used to estimate breeding phenology (number of pairs monitored by year), breeding success (number of pairs monitored by year) and number of age 0 sandeel measured from puffin diet samples used in the sandeel Gompertz Growth Model.

Year	Razorbill		Guillemot		Puffin			Kittiwake		Shag	
	Phenology	Breeding success	Phenology	Breeding success	Phenology	Breeding success	age 0 sandeels	Phenology	Breeding success	Phenology	Breeding success
1999	122	141	828	871	29	181	1441	101	156	57	57
2000	121	147	874	931	23	132	1712	85	97	125	125
2001	155	167	941	973	40	185	1853	116	116	134	134
2002	154	167	942	955	44	174	1590	158	161	129	129
2003	156	177	990	1014	43	195	2204	88	88		
2004	181	190	958	984	34	196	3395	162	162	112	112
2005	182	194	899	935	55	184	2699	224	225	43	43
2006	186	190	911	932	42	166	2029	198	198	79	79
2007	176	188	838	850	45	158	1525	193	193	56	56
2008	169	170	778	806	103	179	918	166	166	60	60
2009	177	183	794	823	71	176	1085	143	143	57	57
2010	167	176	823	847	101	169	1226	165	165	72	72
2011	170	176	809	838	114	173	1685	156	162	102	102
2012	185	196	811	812	43	167	2198	170	171	107	107
2013	188	191	761	797	89	163	1491	118	119	54	54
2014	208	212	812	826	80	192	1330	144	144	54	54
2015	209	218	897	914	63	193	1943	192	196	56	56
2016	209	211	944	972	69	186	2434	139	141	51	51

Text S3. Sandeel growth model

Model specifications

For individual i, $obsTL_{it}$ (in mm) was the total length measured at time t (day of the year). Growth was modelled using a Gompertz Growth Function (GGF, Fig. S1) to describe TL_{it}. An error term accounting for both potential measurement error and deviation from the GGF was incorporated to relate the $obsTL_{it}$ to TL_{it}, similar to the formulation in Reinke et al. (2020). A normal error structure was used with:

$$obsTL_{it} \sim Normal\left(TL_{it}, {\sigma^2}_{sampler}\right) \quad (1)$$

where ${\sigma^2}_{sampler}$ is a gear-specific variance. Gear-specific standard deviations (accounting for sampling error and lack of fit of the GGF with the observed sizes) were small for gears that target larvae (Methot net, Gulf III sampler, and 1m-ringnet) and for dredges as well as puffin chick diet. Due to the relatively small number of observations, standard deviations for grabs and pelagic trawls were much larger. The GGF formulation adopted here uses four parameters. $L0$ is an offset value corresponding to size at hatching, $Linf_i$ is the asymptotic size, K_i is a growth rate coefficient and Ti is the date (day of the year) of the inflection point used as a proxy for settlement. The latter two parameters are affected by asynchrony of sandeel with their copepod

prey, and therefore, allow the GGF model to incorporate the influence of age 0 sandeel trophic interactions with their prey (Régnier et al. 2017, 2019). The GGF is formulated as:

$$TL_{it} = L0 + Linf_i \times exp\,(-exp(-K_i \times (t_i - Ti_i))) \quad (2)$$

The parameters Ti_i, $Linf_i$ and K_i were estimated at the individual level while initial size, $L0$, was assumed to be constant. We assumed a normal distribution restricted to be positive for parameters $Linf_i$ and Ti_i with:

$$Linf_i \sim Normal\left(\mu_{Linf} + y_{Linf_{year}}, \sigma^2{}_{Linf}\right) \quad (3)$$

$$Ti_i \sim Normal\left(\mu_{Ti} + y_{Ti_{year}}, \sigma^2{}_{Ti}\right) \quad (4)$$

A logit-normal variation was assumed for the growth rate K_i, with:

$$logit(K_i) \sim Normal\,(\mu_K + y_{K_{year}}, \sigma^2{}_K) \quad (5)$$

Weakly informative priors were used for μ_{Linf} and μ_{Ti}, with μ_{Linf} ~Normal(77,100) centred on the average length of age 0 sandeel observed in winter dredge surveys and μ_{Ti} ~Normal(130,100), centred on approximate date at settlement (Gibb et al. 2017, Régnier et al. 2017). A semi-informative prior was used for $L0$ with μ_{L0} ~Normal(6,2) based on observed length at hatching in *A. marinus* (Régnier et al. 2018). For μ_K, a vague prior was used with μ_K ~Normal(0,1000). Priors for year-specific parameters $yLinf_{year}$ and yTi_{year} were assigned to a normal distribution centred on 0 with a large variance (Normal(0,1000) while yK_{year} was given a semi informative prior with yK_{year} ~Normal(0,0.1)). For parameters $\sigma_{sampler}$ and σ_{Ti}, t-distributed priors were used with σ ~ t(0,0.0004,3) restricted to be positive. For σ_{Linf} and σ_K, truncated positive Normal distributions were used (means 10 and 0.1, variances 0.25 and 0.001 respectively). A total of 300,000 iterations with an adaptive phase of 50,000 iterations, a burn-in of 50,000 iterations and 200,000 iterations were used to estimate the posterior distributions of the parameters with 2 parallel chains. Convergence was assessed visually through trace-plots and analytically through the potential scale reduction factor (PSRF, Gelman & Rubin 1992) for which an upper 0.975 quantile of <1.2 has been given as a rule of thumb to indicate convergence (Smith 2007). The program JAGS (Plummer 2003) was used to run the model through an R interface (R 4.1.2, R Core Team 2021) using the *rjags* package. Goodness of fit was assessed visually for each year plotting observations, annual mean and individual predictions.

Model outputs

Convergence was achieved for all model parameters presented in Fig. 2 in the main text, and the model provided a good fit to the data overall (Fig. S2). Sampling processes unaccounted for in the model led to localised lacks of fit (e.g. year 2010, Figs. S2-S3) but had minor effects on the predictive power of the model. In particular, age 0 sandeel lengths obtained from puffin chick diet showed a decrease throughout July (starting around day 180 where day 1 = 1 Jan) in a number of years, leading to estimated sizes being larger than observations for these periods (Fig. S3). This apparent lack of large age 0 sandeel toward the end of the chick rearing period in puffin is consistent with a condition-dependent decrease in sandeel activity and coincided with the time age 0 sandeel reached their asymptotic size during their first year (Fig. S3). This observation supports the use of the date at which age 0 sandeel reached 95% of their asymptotic size as a proxy for the end of the period of age 0 availability.

The main parameters of interest (K, $Linf$ and Ti) were only weakly correlated with all correlation coefficients in the range -0.06 to 0.29. Settlement date (Ti) was positively related to sandeel hatching date ($R^2 = 0.57$, $F_{1,15} = 19.78$, $p=0.0005$, Fig. S4), such that later hatching translated into later settlement. The growth rate parameter (K) increased with average sea temperature in the 60 days following sandeel hatching and with the measure of synchrony

between sandeel and their copepod prey (Régnier et al. 2019) but decreased with their interaction (Fig. S5). In particular, the positive effect of temperature on growth rate was associated with good synchrony between sandeel and their prey, while the cost of trophic asynchrony on growth rate became apparent at high temperatures (Fig. S5). Estimates of *sandeelSTART* and *sandeel END* were related to the estimated growth rate and date of settlement (Fig. S6).

Our ability to identify trophic linkages, which propagated from lowest trophic levels to seabird predators, depended on an accurate description of age 0 sandeel (*A. marinus*) growth. The Gompertz Growth Model (GGM) used multiple data sources allowing a good coverage of the juvenile period and was validated by a good fit of the individual growth trajectories to the data. This model enabled the estimation of key parameters of age 0 sandeel growth and phenology, necessary for the study of trophic mismatch with their avian predators. The twofold variation of the estimated age 0 sandeel growth in the 17-year time-series was best explained by an interaction between trophic asynchrony with their copepod prey and average temperature in the 2 months following hatching. As the trophic asynchrony between age 0 sandeel and their copepod prey is itself indirectly related to temperature (Régnier et al. 2019), age 0 sandeel growth is therefore temperature sensitive and a parameter of interest in the context of climate change. In terms of phenology, the date of settlement and the date at which sandeel reach 50 mm and appeared in seabird diet could be estimated and marked the start of the period of age 0 sandeel availability. Estimated dates of settlement were within the range of settlement dates back-calculated from age 0 otoliths (Gibb et al. 2017). Year-specific values from the two methods were positively correlated confirming that the date of the inflection point in the growth model was an appropriate proxy for settlement date. There was also a strong relationship between this parameter, hatching dates estimated from otoliths and the appearance of larvae (Régnier et al. 2017, 2019), providing further confidence in the use of these parameters. As our measure of age 0 sandeel availability integrates prey quality by reflecting the availability of age 0 sandeel of a size > 50 mm, some years were characterised by a very short period of age 0 sandeel availability (e.g. 2007, Fig. 2a in the main text). For such years, while age 0 sandeel were present in seabird diets, the fish from puffins were very small and the corresponding energetic content and profitability would have been very low (Hislop et al. 1991). The assumption that, as in older sandeel, availability of age 0 sandeel decreased as a trade-off between growth opportunity and predation risk (Haynes et al. 2007, Bergstad et al. 2002) was supported by the data. A decrease in the size range of age 0 sandeel caught by puffins coincided with the date age 0 sandeel reached their maximum size during the first summer (Fig. S3). Both the estimated dates of the start and end of the period of age 0 sandeel availability were defined by variability in the date of settlement and growth rate (Fig. S6). As growth in ectotherms is sensitive to temperature, age 0 sandeel phenology and the degree of synchrony between age 0 sandeel availability and seabird breeding phenology are therefore likely influenced by climate change. Fig S7 shows the measure of overlap between age 0 sandeel availability and seabird chick-rearing period was related to both the date of the start and end of the period of age 0 sandeel availability.

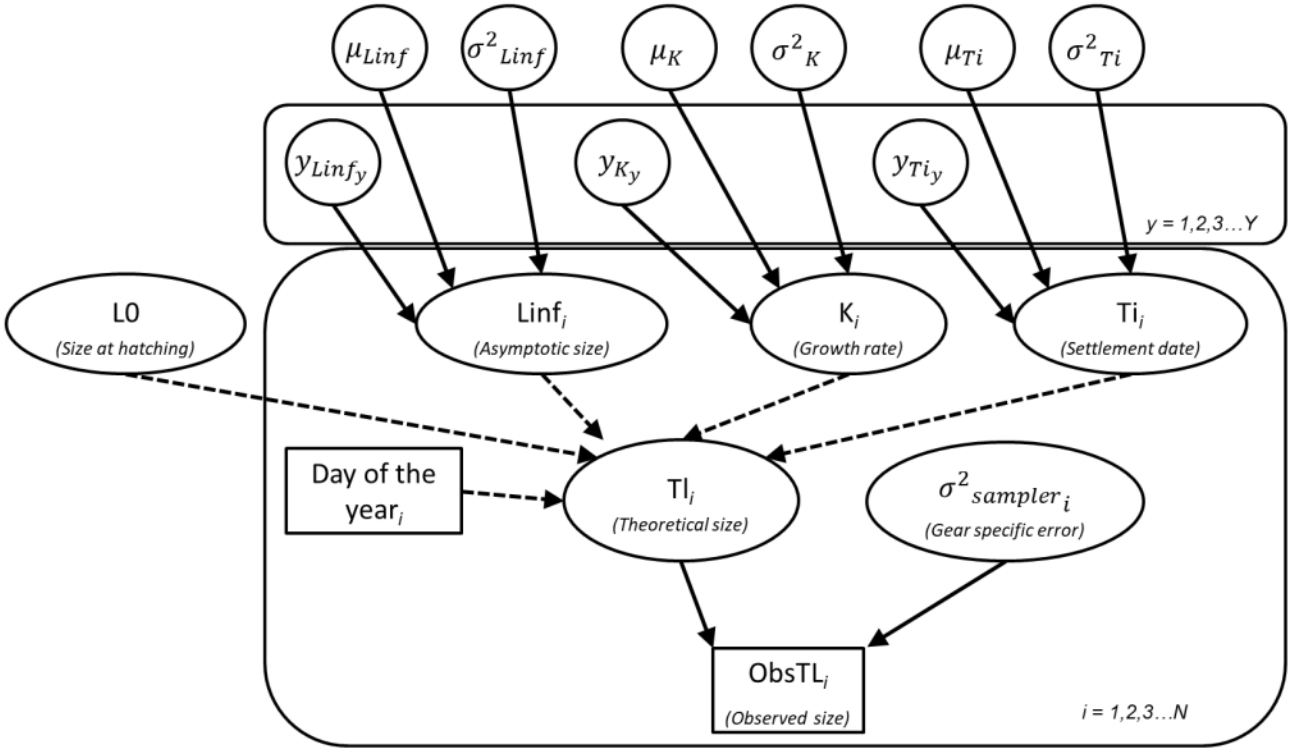

Fig. S1. Directed Acyclic Graph (DAG) corresponding to the sandeel growth model. Squares denote constants, circles denote variables. Solid arrows denote stochastic processes while dotted arrows denote deterministic processes.

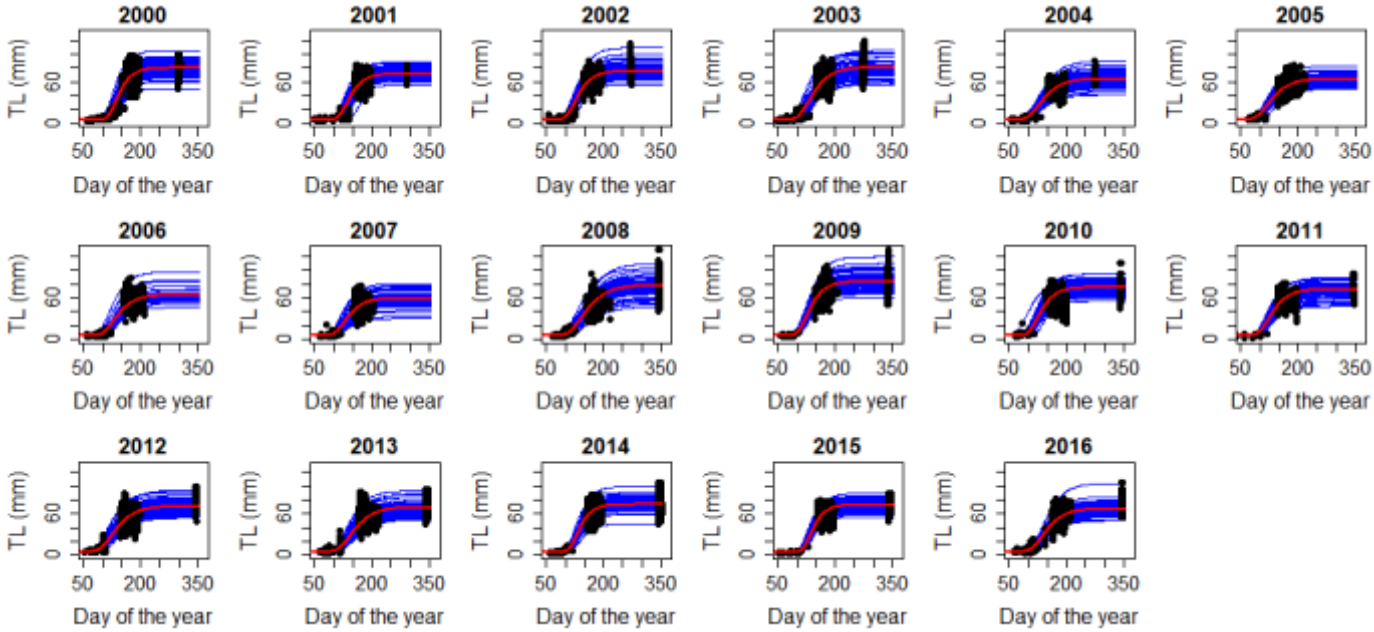

Fig. S2. Estimated trajectories for age 0 sandeel for years 2000 to 2016. Individual data are indicated in black, solid red lines correspond to the annual trajectories and solid blue lines correspond to individual trajectories for a sample of 150 individuals each year.

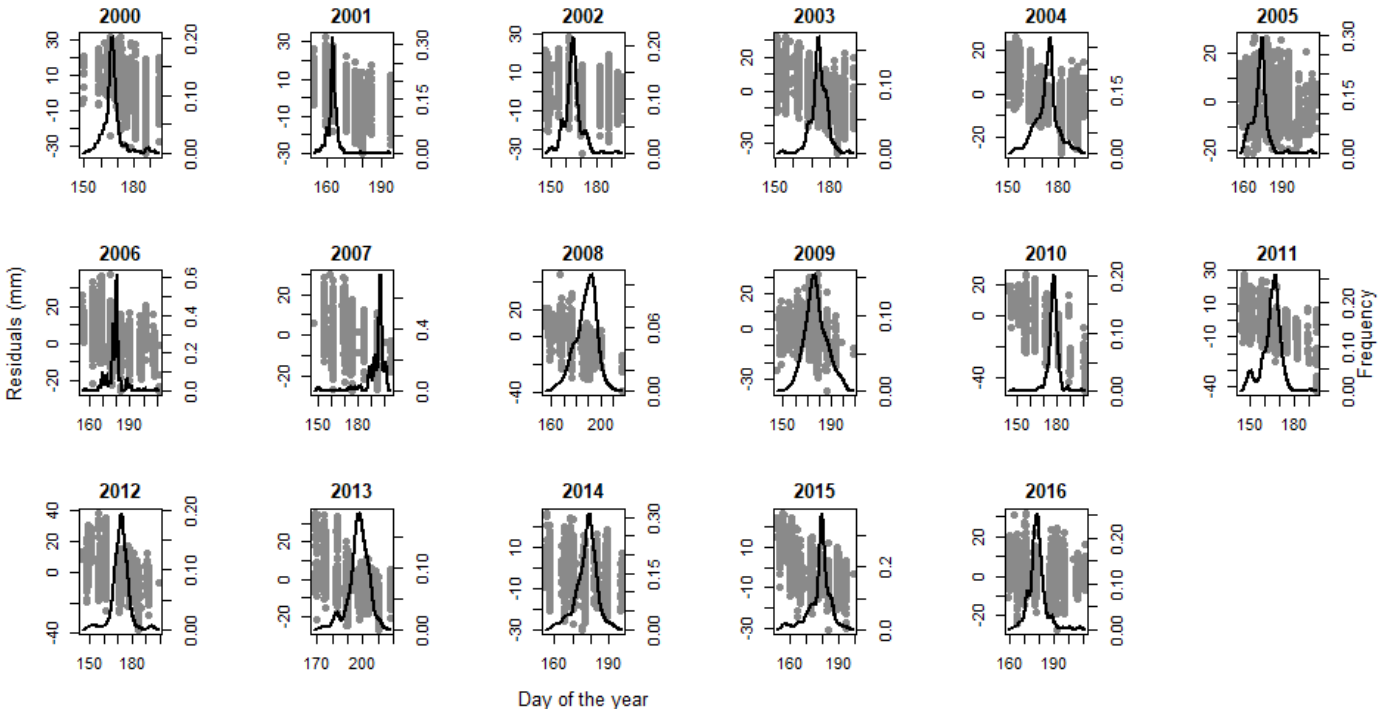

Fig. S3. Deviations between sizes of age 0 sandeel captured by puffins and predictions from the Age 0 growth model (grey points, left axis). The density distribution of the end of sandeel availability is indicated by a thick line (black, right axis).

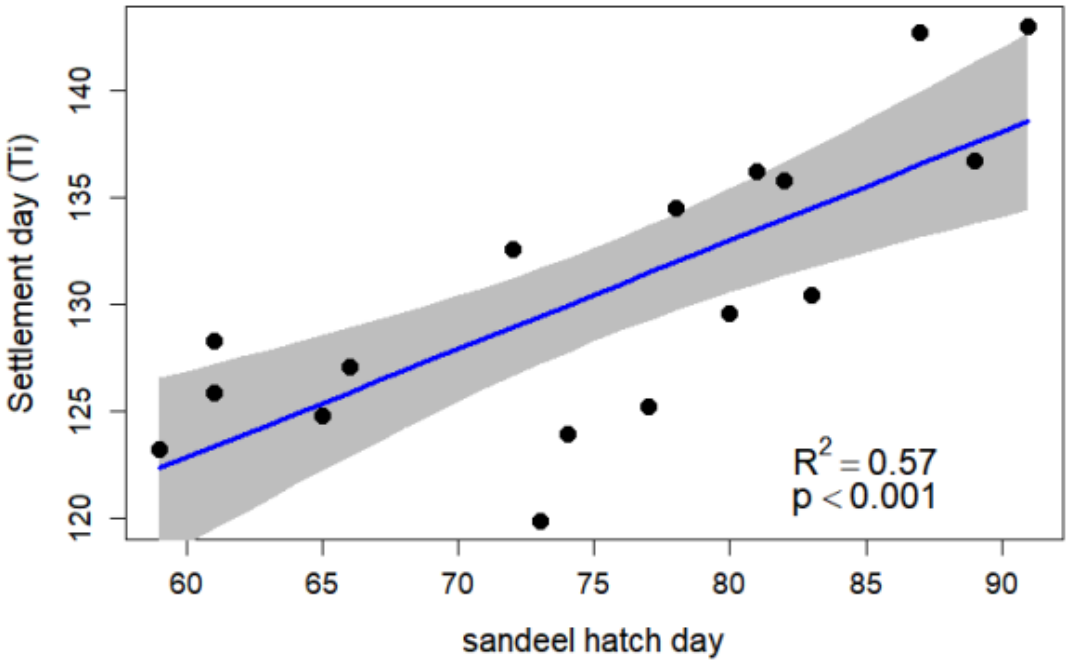

Fig. S4. Relationship between settlement date (parameter Ti) and median hatch day estimated for sandeel from Régnier et al. (2019). The mean response is indicated by a solid line and the 95% confidence interval is shaded.

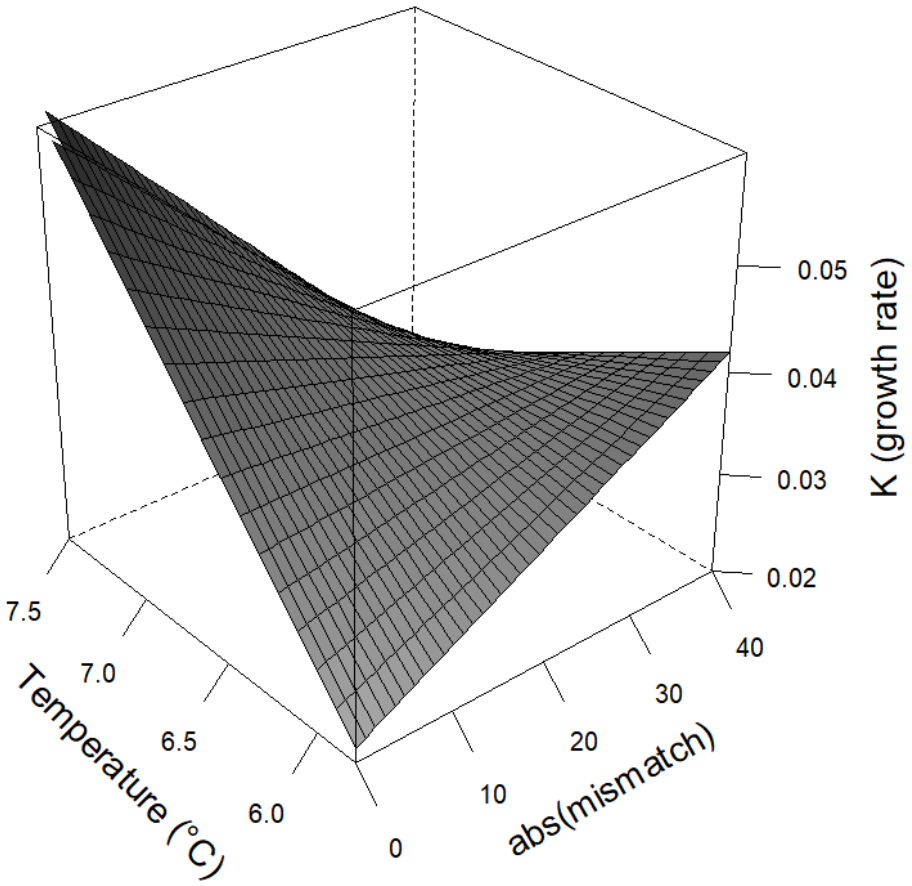

Fig. S5. Relationship between average sea temperature (°C), estimated growth rate [K] and the degree of trophic mismatch between *Ammodytes marinus* and its copepod prey (absolute value).

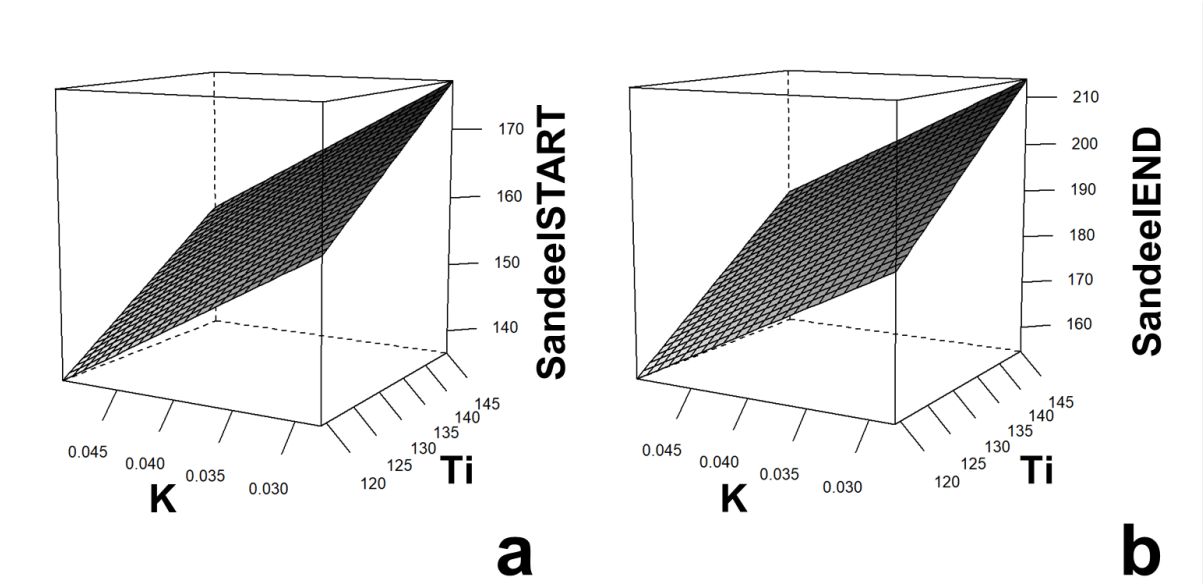

Fig. S6. Relationship between (a) the start of the period of age 0 sandeel availability and the estimated growth rate [K] and date of settlement [Ti] and (b) the end of the period of age 0 sandeel availability and the estimated growth rate [K] and date of settlement [Ti].

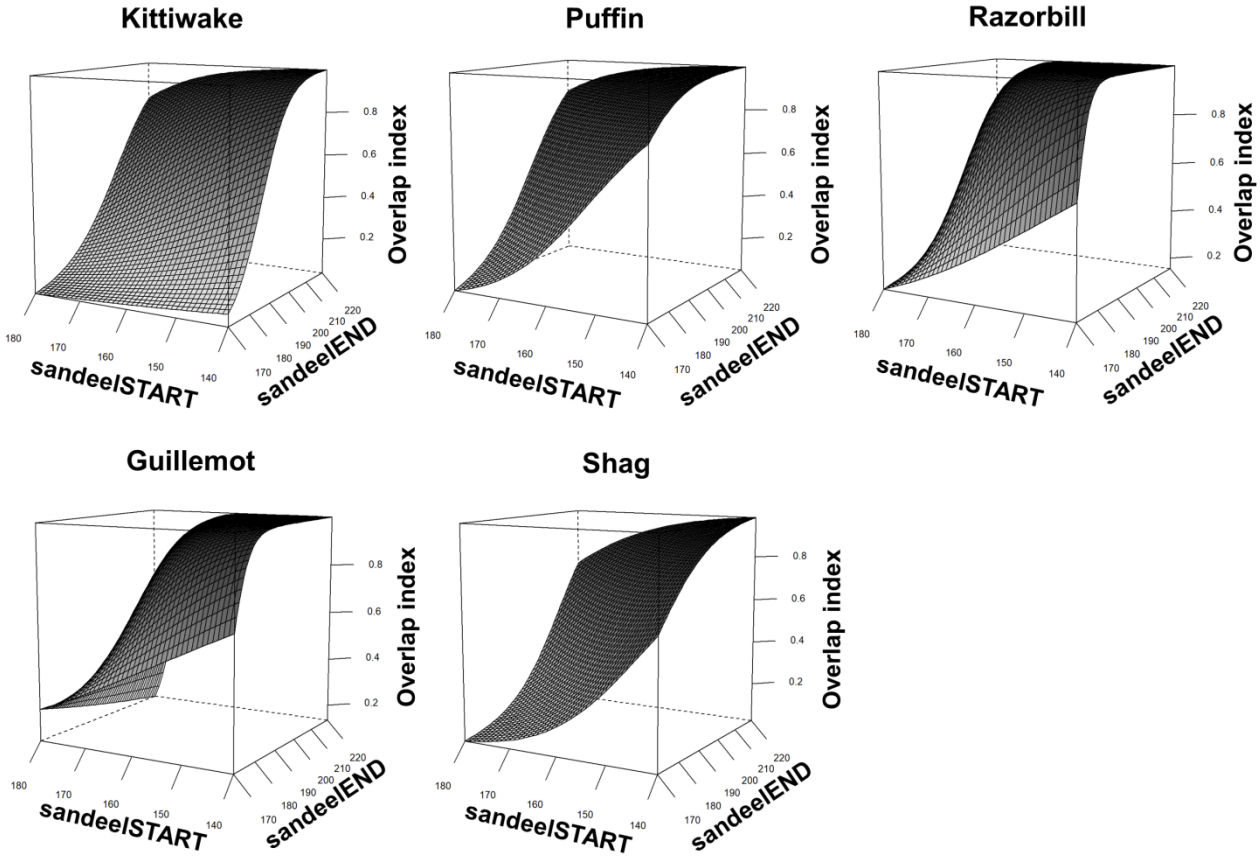

Fig. S7. Relationship between the overlap between the chick rearing period (overlap index) and the date of the start and end of the period of age 0 sandeel availability for the five seabird species considered.

LITERATURE CITED

Bergstad OA, Høines ÅS, Jørgensen T (2002) Growth of sandeel, *Ammodytes marinus*, in the northern North Sea and Norwegian coastal waters. Fish Res 56:9–23 doi: 10.1016/S0165-7836(01)00317-4

Gelman A, Rubin DB (1992) Inference from iterative simulation using multiple sequences. Stat Sci 7: 457– 472 doi: 10.1214/ss/1177011136

Gibb FM, Régnier T, Donald K, Wright PJ (2017) Connectivity in the early life history of sandeel inferred from otolith microchemistry. J Sea Res 119:8–16 doi: 10.1016/j. seares.2016.10.003.

Harris MP, Wanless S (2011) The Puffin. T & AD Poyser, London

Haynes TB, Ronconi RA, Burger AE (2007) Habitat use and behavior of the pacific sand lance (*Ammodytes Hexapterus*) in the shallow subtidal region of southwestern Vancouver Island. Northwest Nat 88:155–167 doi: 10.1898/1051-1733(2007)88[155:HUABOT] 2.0.CO;2

Hislop JRG, Harris MP, Smith JGM (1991) Variation in the calorific value and total energy

content of the lesser sandeel (*Ammodytes marinus*) and other fish preyed on by seabirds. J Zool 224:501–517 doi: 10.1111/j.1469-7998.1991.tb06039.x

ICES (2021) Herring Assessment Working Group for the Area South of 62° N (HAWG). ICES Sci Rep 3:12. 917pp. doi:10.17895/ices.pub.8214

Newell M, Wanless S, Harris MP, Daunt F (2015) Effects of an extreme weather event on seabird breeding success at a North Sea colony. Mar Ecol Prog Ser 532:257–268 doi:10.3354/meps11329

Plummer M (2003) JAGS: A program for analysis of Bayesian models using Gibbs sampling. In: Hornik K, Leisch F, Zeileis A (eds) Proceedings of the 3rd international workshop on distributed statistical computing, 124:1–10. Technische Universität Wien, Vienna, Austria Available from: https://www.r-project.org/conferences/DSC-2003/Proceedings/Plummer.pdf

R Core Team (2021) R: A Language and Environment for Statistical Computing. R Foundation for Statistical Computing, Vienna. https://www.r-project.org

Régnier T, Gibb FM, Wright PJ (2017) Importance of trophic mismatch in a winterhatching species: evidence from lesser sandeel. Mar Ecol Prog Ser 567:185–197 doi: 10.3354/meps12061

Régnier T, Gibb FM, Wright PJ (2018) Temperature effects on egg development and larval condition in the lesser sandeel, *Ammodytes marinus*. J Sea Res 134:34–41 doi: 10.1016/j.seares.2018.01.003

Régnier T, Gibb FM, Wright PJ (2019) Understanding temperature effects on recruitment in the context of trophic mismatch. Sci Rep 9:15179 doi: 10.1038/s41598-019-51296-5

Reinke BA, Hoekstra L, Bronikowski AM, Janzen FJ, Miller D (2020) Joint estimation of growth and survival from mark-recapture data to improve estimates of senescence in wild populations. Ecology 101:e02877 doi:10.1002/ecy.2877

Wanless S, Harris MP, Newell MA, Speakman JR, Daunt F (2018) Community-wide decline in the occurrence of lesser sandeels *Ammodytes marinus* in seabird chick diets at a North Sea colony. Mar Ecol Prog Ser 600:193-206 doi: 10.3354/meps12679